


Different Molecular Mechanisms Mediate Direct or Glia-Dependent Prion Protein Fragment 90–231 Neurotoxic Effects in Cerebellar Granule Neurons

Stefano Thellung¹ · Elena Gatta² · Francesca Pellistri² · Valentina Villa¹ · Alessandro Corsaro¹ · Mario Nizzari¹ · Mauro Robello² · Tullio Florio¹ 

Received: 8 August 2016 / Revised: 2 May 2017 / Accepted: 4 May 2017 / Published online: 25 May 2017
© Springer Science+Business Media New York 2017

Abstract Glia over-stimulation associates with amyloid deposition contributing to the progression of central nervous system neurodegenerative disorders. Here we analyze the molecular mechanisms mediating microglia-dependent neurotoxicity induced by prion protein (PrP)^{90–231}, an amyloidogenic polypeptide corresponding to the protease-resistant portion of the pathological prion protein scrapie (PrP^{Sc}). PrP^{90–231} neurotoxicity is enhanced by the presence of microglia within neuronal culture, and associated to a rapid neuronal $[Ca^{++}]_i$ increase. Indeed, while in “pure” cerebellar granule neuron cultures, PrP^{90–231} causes a delayed intracellular Ca^{++} entry mediated by the activation of NMDA receptors; when neuron and glia are co-cultured, a transient increase of $[Ca^{++}]_i$ occurs within seconds after treatment in both granule neurons and glial cells, then followed by a delayed and sustained $[Ca^{++}]_i$ raise, associated with the induction of the expression of inducible nitric oxide synthase and phagocytic NADPH oxidase. $[Ca^{++}]_i$ fast increase in neurons is dependent on the activation of multiple pathways since it is not only inhibited by the blockade of voltage-gated channel activity and NMDA receptors but also prevented by the inhibition of nitric oxide and PGE₂ release from glial cells. Thus, Ca^{++} homeostasis alteration, directly induced by PrP^{90–231} in cerebellar granule

cells, requires the activation of NMDA receptors, but is greatly enhanced by soluble molecules released by activated glia. In glia-enriched cerebellar granule cultures, the activation of inducible nitric oxide (iNOS) and NADPH oxidase represents the main mechanism of toxicity since their pharmacological inhibition prevented PrP^{90–231} neurotoxicity, whereas NMDA blockade by D(–)-2-amino-5-phosphonopentanoic acid is ineffective; conversely, in pure cerebellar granule cultures, NMDA blockade but not iNOS inhibition strongly reduced PrP^{90–231} neurotoxicity. These data indicate that amyloidogenic peptides induce neurotoxic signals via both direct neuron interaction and glia activation through different mechanisms responsible of calcium homeostasis disruption in neurons and potentiating each other: the activation of excitotoxic pathways via NMDA receptors and the release of radical species that establish an oxidative *milieu*.

Keywords Prion protein · Neuronal death · Microglia · Astrocytes · Nitric oxide · $[Ca^{++}]_i$ · NMDA

Introduction

Protein misfolding represents the molecular basis of both high (Alzheimer and Parkinson diseases) and low incidence neurodegenerative disorders (i.e., transmissible spongiform encephalopathies or prion diseases) (Diack et al. 2016; Forloni et al. 2016). Human prion diseases are paradigmatic of proteinopathies because their onset is correlated with the post-translational misfolding of a host-encoded glycoprotein (named cellular prion protein or PrP^C) into an amyloidogenic and protease-resistant conformer (prion protein scrapie or PrP^{Sc}) (Prusiner 1998). PrP^{Sc} generation represents the unifying pathogenic trait for prion diseases occurring in humans (Creutzfeldt-Jakob disease,

Stefano Thellung, Elena Gatta, and Francesca Pellistri equally contributed to this study, and all should be considered as first authors.

✉ Tullio Florio
tullio.florio@unige.it

¹ Laboratory of Pharmacology, Department of Internal Medicine, and Center of Excellence for Biomedical Research (CEBR), University of Genova, 16132 Genoa, Italy

² Department of Physics, University of Genova, Genoa, Italy

Gerstmann-Sträussler-Scheinker disease, fatal familial Insomnia, Kuru) or animals (ovine scrapie and bovine spongiform encephalopathy, among others), otherwise heterogeneous as far as host, etiology (sporadic, familial and infectious), neuropathology, and symptomatology (Corsaro et al. 2012b; Ghetti et al. 1995; Liberski et al. 2012; Montagna et al. 2003; Puoti et al. 2012). PrP^C => PrP^{Sc} transition may occur stochastically, as in sporadic forms, driven by familial mutations of the PrP-encoding gene (*PRNP*), or as result of infective processes caused by the interaction-refolding between PrP^C and exogenous PrP^{Sc}, with PrP^{Sc} acting as template (Caughey 2003; Jucker and Walker 2013; Soto et al. 2006). How PrP^C misfolding into PrP^{Sc} may lead to gray matter vacuolation, neuronal loss and gliosis, the main pathological hallmarks of prion diseases, is still not completely defined. Different theories were proposed, involving either the loss of neuroprotective function of PrP^C or the gain of neurotoxicity by PrP^{Sc} (Chiesa 2015). Noteworthy, amyloid fibrils and plaques containing PrP^{Sc} have been described within gray matter in association with tissue vacuolation, glial proliferation and neuronal loss (Bruce et al. 1989; DeArmond et al. 1987) supporting the hypothesis that misfolded oligomeric species, arising from PrP^{Sc} formation may produce neuronal apoptosis and gliosis (Chiovitti et al. 2007; Mallucci et al. 2007; Novitskaya et al. 2006).

This hypothesis further links prion neurotoxicity to Alzheimer disease in which amyloid-beta (A β) peptides have been proposed to induce neuronal death as soluble monooligomers (Kayed et al. 2003; Kim et al. 2003); importantly, the occurrence of similar mechanisms of neurodegeneration in different proteinopathies supports the search for common therapeutic approaches for all the neurodegenerative conditions caused by protein misfolding (Aguzzi and O' Connor 2010; Monaco et al. 2006; Tousseyn et al. 2015). Gliosis involves the proliferation of reactive astrocytes and the recruitment of activated microglia representing a constant histopathological feature in brain areas displaying neurodegeneration. Moreover, gliosis is frequently observed in close vicinity or in direct association with PrP^{Sc} or A β aggregates in patients or in animal models of Alzheimer's and prion diseases (Bugiani et al. 2000; Guirouy et al. 1994; Miyazono et al. 1991; Serrano-Pozo et al. 2011).

While astrocytes play a pivotal role in maintaining brain homeostasis providing trophic support to neurons and buffering neurotransmitter release, microglial cells represent the effectors of innate immunity within CNS removing pathogens, dying cells, and misfolded proteins (Aguzzi et al. 2013). Microglia activation follows PrP^{Sc} deposition and contributes to neuronal apoptosis (Betmouni et al. 1996; Williams et al. 1997). In particular, activation of phagocytic microglia contributes to lower the burden of amyloid proteins in CSN (Koenigsnecht and Landreth 2004; Mandrekar et al. 2009), but, if over-activated, it can also exacerbate neurotoxic processes and thus is now considered a novel pharmacological

target (McGeer and McGeer 2015). Amyloid-activated microglia was reported to induce synapse loss (Hong et al. 2016), direct neuron phagocytosis (Neniskyte et al. 2011), or persistent production of oxidative molecules (Fiala et al. 2007; Weldon et al. 1998). In particular, superoxide anion (O₂⁻) generated by phagocytic NAPH oxidases (Bedard and Krause 2007) and nitric oxide (NO) by inducible nitric oxide (iNOS) represent the main mediators of glia-induced oxidative stress in neurons (Haas et al. 2002). Synaptic rarefaction in Alzheimer and prion diseases is associated to neuronal oxidative stress, involving DNA oxidation, protein nitrosylation and lipid peroxidation caused by sustained activation of microglial cells. Microglia also contribute to maintain an oxidizing extracellular milieu that eventually will favor further PrP^{Sc} (or A β) deposition and neuronal death (Guentchev et al. 2002; Leszek et al. 2016; Van Everbroeck et al. 2004). In fact, in both Alzheimer and prion diseases, reactive microglia contains intralysosomal deposits of pathological misfolded proteins (Jeffrey et al. 1994; Xie et al. 2013).

In vitro, different amyloidogenic peptides derived from both A β and PrP^{Sc} were reported to induce neuronal death and glial cell over-activation; thus, they are widely used to model the mechanisms of neurotoxicity in naturally occurring proteinopathies and challenge the feasibility of therapeutic strategies, at least as proof of principle (Chabry et al. 2003; Corsaro et al. 2009; Corsaro et al. 2012a; Florio et al. 1996; Fluharty et al. 2013; Forloni 1996; Post et al. 2000; Scorziello et al. 1996; Selkoe and Hardy 2016). To this aim, we used an amyloidogenic polypeptide matching human prion protein 90–231 amino acid sequence laying within the protease-insensitive core of PrP^{Sc} (Notari et al. 2008; Xiao et al. 2014), synthesized as recombinant protein (Corsaro et al. 2002). We demonstrated that PrP90–231 induces both functional activation of type I astrocytes and microglial cells (Thellung et al. 2007b; Villa et al. 2016a, b) and apoptosis in neuronal cells (Corsaro et al. 2006; Corsaro et al. 2011; Thellung et al. 2011). Importantly, PrP90–231 treatment causes similar membrane ion currents in neuronal models than brain purified pathological PrP^{Sc} (Paulis et al. 2011; Sorrentino et al. 2012). We previously characterized the mechanisms of PrP90–231 neurotoxicity in primary cultures of cerebellar granules, focusing on the alteration of Ca⁺⁺ homeostasis (Thellung et al. 2013), reporting that prolonged exposure (24 h) to PrP90–231, but not acute treatment, induced a sustained elevation of intracellular Ca⁺⁺ concentration ([Ca⁺⁺]_i) in cerebellar neurons. This effect was mediated by the activation of NMDA and α -amino-3-hydroxy-5-methyl-4-isoxazolepropionic acid (AMPA) receptors, since their pharmacological inhibition prevented the [Ca⁺⁺]_i increase induced by PrP90–231 and the consequent neurotoxicity. These experiments were performed on “pure” cerebellar granule cultures in which the addition of the antiproliferative drug cytosine arabinoside (Ara-C) (Thellung et al. 2000b) restrains type I

astrocytes content below 5% and microglial cells to almost undetectable levels (about 0.3%). The toxicity of PrP90–231 in purified granule cultures suggests that the peptide produces a long-lasting disruption of $[Ca^{++}]_i$ homeostasis through activation of NMDA receptors; on the other hand, the low content of astrocytes and microglial cells hinders glial-mediated neurotoxic pathways that may actually be activated by PrP90–231.

The present work is aimed to characterize the molecular mechanisms of contribution of glial cells in the toxic effects of PrP90–231 in cerebellar granule neurons using a more integrated cellular model to better mimic glia recruitment and activation by neurotoxic amyloidogenic peptides. We established glia/neuron mixed cultures allowing the proliferation of astrocytes and microglia within cerebellar primary cultures by delaying the addition of Ara-C. In this way, we increased astrocyte and microglia content up to 15 and 5% of total cells, respectively. PrP90–231 reduces granule cell viability much more efficiently in the presence of glia than in pure granular neuron cultures. The presence of glia increased the expression of ROS-producing enzyme phagocytic NADPH oxidase (PHOX) and the upregulation of inducible nitric oxide synthase (iNOS); the relevance of reactive species of oxygen and nitrogen in PrP90–231 neurotoxicity is demonstrated by its reversal by PHOX and iNOS pharmacological inhibition. Importantly, in the presence of glia, we registered an immediate Ca^{++} response in both neurons and glial cells: in about 70% of glial cells and in 20% of granule cells the stimulation with PrP90–231 elicited a rapid increase of $[Ca^{++}]_i$; that, in pure cerebellar granule cells (CGCs), we did not record. These data indicated that the presence of reactive glia might increase the sensitivity of granule neurons to the Ca^{++} -dependent signaling of PrP90–231. However, in these experimental conditions, microglia inhibition, but not NMDA blockade, was sufficient to protect granules from PrP90–231 neurotoxicity, suggesting that the presence of glia causes the activation of oxidative neurotoxic pathways that damages neurons beyond the excitotoxic pathway. These data highlight the interaction between direct, NMDA-dependent and glia-dependent, oxidative PrP90–231 neurotoxicity, and indicate that neuronal sensitivity to Ca^{++} homeostasis alteration is enhanced by radical species released from activated glial cells.

Materials and Methods

Chemicals

The 3-(4,5-dimethylthiazol-2-yl)-2,5-diphenyltetrazolium bromide (MTT), iNOS inhibitors *N*- ω -nitro-L-arginine (NNA) and W1400, PHOX inhibitor apocynin, and NMDA antagonist D(-)-2-amino-5-phosphonopentanoic acid (AP-V) were purchased from Sigma-Aldrich (Milano, Italy). Fluorescent probe Oregon Green was purchased from

Molecular Probes-ThermoFisher (Monza, Italy). Primary antibodies against iNOS, NOX2, GFAP, CD11b (OX42), aldehyde 4-dihydroxynonenal (HNE), and β III-tubulin were from Abcam (Cambridge, UK), and secondary antibodies and DAPI for nuclear staining were from Molecular Probes-ThermoFisher.

Purification and β -Refolding of PrP90–231

PrP90–231 was obtained and purified as previously described (Corsaro et al. 2002) and stored at $-80^\circ C$, up to 30 days from the purification. Before experiments, PrP90–231 was incubated for 1 h $53^\circ C$ to induce thermal denaturation misfolding into a β -structure-rich isoform (Chiovitti et al. 2007; Corsaro et al. 2006). Therefore, throughout the paper, the term PrP90–231 indicates the misfolded isoform of the peptide. Cell treatments were performed adding PrP90–231 directly to the culture medium.

Primary Cultures

CGCs were obtained from 7-day-old Sprague-Dawley rat cerebella as previously described (Gatta et al. 2010; Piccioli et al. 2001) and plated on poly-L-lysine-coated plastic or glass coverslips. Cultures were grown in basal Eagle's medium supplemented with 10% fetal calf serum (Sigma-Aldrich) KCl 25 mM, glutamine 2 mM, and gentamicin 100 $\mu g/ml$, and kept at $37^\circ C$ in 5% CO_2 humidified atmosphere. To obtain purified CGCs, 10 μM Ara-C was added to the culture medium after 24 h to prevent the proliferation of glial cells. To prepare glia-enriched CGCs, Ara-C was added after 5 days in vitro (DIV). Treatments with PrP90–231 were initiated at 7 DIV. Experimental procedures and animal care complied with the EU Parliament and Council Directive of 22 September 2010 (2010/63/EU) and were approved by the Italian Ministry of Health (protocol number 2207-1) in accordance with D.M. 116/1992. All efforts were made to minimize animal suffering and to reduce the number of animal used.

$[Ca^{++}]_i$ Measurement

Cells were incubated in standard external solution (135 mM NaCl, 5.4 mM KCl, 1.8 mM $CaCl_2$, 1 mM $MgCl_2$, 5 mM HEPES, 10 mM glucose, pH 7.4), and probed with 6 μM Oregon Green AM ester (OG) (Molecular Probes, Eugene, OR, USA) at $37^\circ C$ for 40 min. Then, cultures were transferred to a recording chamber mounted onto a Nikon Eclipse TE300 and OG fluorescence was detected in living cells using a Hamamatsu digital CCD camera with a 450/490-nm excitation filter and a 520 nm emission filter (Nikon Italia, Firenze, Italy) (Pellistri et al. 2008). Images were acquired with the Simple PCI software (Compix Imaging Systems, Hamamatsu Corp., Sewickley, PA, USA). Fluorescence

intensity was calculated in arbitrary units by building a scale of the pixel intensity and expressed as percent of increase on a baseline obtained from untreated cells or as percent of cells showing fluorescence increase. The fluorescence of at least 40 cells was analyzed to obtain an average of the signal in each condition.

Cell Viability by MTT Assay

Mitochondrial function, as index of cell viability, was evaluated measuring the intracellular reduction of MTT (Sigma-Aldrich) to a purple formazan by mitochondrial dehydrogenase (Thellung et al. 2000a). Briefly, 0.25 mg/ml MTT was added to culture medium and incubated at 37 °C; after 2 h, medium was removed and formazan crystals were dissolved in dimethylsulfoxide. Absorbance was measured spectrophotometrically at 570 nm using microplate reader BioTek ELx800 (Winooski, VT, USA).

Measurement of Nitric Oxide Release

The amount of nitric oxide (NO) released by cells was evaluated measuring the concentration of nitrites in conditioned medium (Arena et al. 2005). Briefly, 5×10^6 cells from purified or glia-enriched CGC cultures were plated into 60 mm² petri dishes and treated with vehicle (PBS) or PrP90–231 (1 μM). Twenty-four and 48 h later, aliquots from conditioned media were cleared of floating cells and debris by centrifugation and mixed with Griess solution (1/4 vol/vol ratio); nitrates contained in cell-conditioned media rapidly react with Griess reagent forming azo dye that is red at absorbance 570 nm with an ELx800 microplate reader (BioTek).

Analysis of Protein Expression

Immunostaining Cells, grown on glass coverslips, were fixed with ice-cold methanol and permeabilized with PBS containing 0.1% Triton X-100. Coverslips were blocked with bovine serum albumin 2% in PBS (PBS-BSA 2%) and incubated with primary antibodies diluted in PBS-BSA 2% for 1 h. Secondary antibodies were AlexaFluor 488 and AlexaFluor 568 goat antisera raised against mouse and rabbit IgG. Immunostained cells were observed using a fluorescence microscope DM2500 equipped with a DCF310FX camera (Leica, Milano, Italy).

Immunoblotting Cytoplasmic fractions were obtained harvesting cells in lysis buffer (NaCl 150 mM, Tris/EDTA 20 mM pH 8, glycerol 10%, NP-40 1%, protease inhibitor cocktail “Complete mini” [Roche Diagnostic, Mannheim, Germany], PMSF 1 mM, orthovanadate 1 mM) and cleared of nuclei by brief centrifugation (1000×g for 5 min at 4 °C) (Corsaro et al. 2003). Protein concentrations were determined

using Bradford assay and normalized in each samples with lysis buffer. Proteins were boiled with Laemmli buffer, size-fractionated on SDS-polyacrylamide electrophoresis, and transferred to polyvinylidene fluoride membranes (pore 0.45 μm, BioRad). Membranes were blocked with PBS containing 0.1% Tween-20 and 2% bovine serum albumin (PBST-BSA) for 1 h. Primary antibodies were diluted in PBST-BSA and incubated with membranes overnight at 4 °C. Membranes were then incubated with horseradish peroxidase-conjugated secondary antibodies (GEHealthcare, UK) for 1 h, and immunoreactivity was detected by enhanced chemiluminescence (Clarity™ Western ECL Substrate GE Healthcare). Immunoreactive signals were quantified by densitometric analysis using ChemiDoc System (Bio-Rad, Milano, Italy) and processed with Image Lab 4.0.1 (Bio-Rad).

Results

Analysis of Glial Content in Partially Purified and Glia-Enriched CGC Cultures

To investigate the mechanisms by which glial cells contribute to PrP90–231 neurotoxicity, we first evaluated the differences of CGC sensitivity to this peptide in the presence of different glia content in the primary cultures. We prepared pure and “glia-enriched” CGC cultures, whose difference in glial content was obtained by adding the mitotic inhibitor Ara-C after 1 or 5 DIV, respectively. We quantified the amount of glial cells in both culture models by immunostaining of specific markers: glial fibrillary acidic proteins (GFAP), as a marker of reactive type I astrocytes, and CD11b receptor (OX42), as microglia marker; nuclear staining with DAPI was used to calculate the total cell number (Fig. 1). Glia content in pure CGC cultures was about 3–5% type I astrocytes and 0.3–0.5% microglial cells (Fig. 1a, b); conversely, glia-enriched cultures contained about 15% of astrocytes and 5% of microglia (Fig. 1c, d). Beyond the expected increased glial cell content, these immunostaining experiments showed that the culturing settings produced shape differences in astrocytes that shifted from a tiny branched profile, resembling the resting state, as observed in the few astrocytes identified in pure CGC cultures, to an enlarged morphology, typical of reactive astrocytes, when glial growth was allowed. The evaluation of microglia morphology was possible only in glia-enriched conditions because in pure CGC cultures the content of these cells was too low to analyze a significant number of cells.

PrP90–231 Neurotoxicity In Vitro Is Enhanced by Glial Cells

Thus, we investigated whether the presence of astrocytes and microglia might affect CGC sensitivity to the neurotoxic

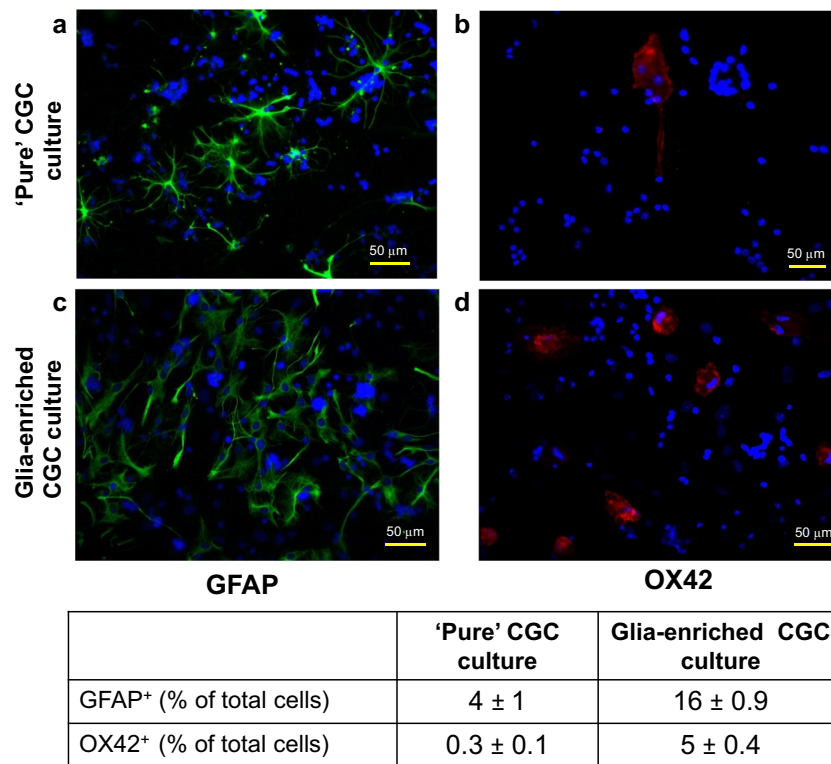


Fig. 1 Analysis of type I astrocytes and microglia percent in “pure” and glia-enriched CGCs. Pure (*upper panels*) and glia-enriched (*lower panels*) CGCs were seeded on glass coverslips for 48 h. Cells were fixed in ice-cold methanol and immunostained with anti-*GFAP* mouse monoclonal antibody (**a, c**) and anti-*CD11b* (*OX42*) mouse monoclonal antibody (**b, d**). Immunoreactivity of *GFAP* and *CD11b* was evidenced with AlexaFluor488 anti-rabbit IgG and AlexaFluor568 anti-mouse IgG

antiserum, respectively; DAPI staining was used to evidence nuclei. Images were obtained by fluorescence microscopy (objective lens: HC PL Fluotar 20X/0.50; *scale bar* = 50 μm). The table below, obtained by counting cells with ImageJ software, reports the percent of *GFAP*- and *CD11b*-positive cells on the total amount of DAPI-reactive nuclei. Values represent the average \pm SEM observed in a 13-mm coverslip from three independent CGC preparations

activity of PrP90–231. To this aim, both pure and glia-enriched CGC cultures were treated with PrP90–231 (1 μM). Cultures were photographed under phase-contrast microscope and cell viability measured by MTT reduction test, after 48 and 72 h.

In line with our previous results (Thellung et al. 2013), exposure of pure CGCs to PrP90–231 for 48 h produced a modest loss of viability, and 72 h of treatment was required to cause a highly significant toxicity (about 35%). In contrast, CGC cultures containing glial cells were highly responsive to PrP90–231 that caused a reduction of cell viability of about 48 and 56%, after 48 and 72 h, respectively (Fig. 2a). Given the heterogeneity of cerebellar granule cultures, particularly when glial proliferation is allowed (neuronal death by PrP90–231 is associated with astrocyte proliferation) (Thellung et al. 2007b), the correct interpretation of the quantitative results of the MTT assay has to be integrated with qualitative analysis of the cellular effects induced by PrP90–231. To this aim, we analyzed phase-contrast microphotographs of both cultures exposed for 72 h to the peptide (Fig. 2b). Comparing glia-enriched CGC cultures with untreated pure CGCs, it is appreciable that the neurite network among granule cells is preserved indicating that the presence of glial cells growing

underneath neurite network is not detrimental for granule neurons survival. In the presence of glia, 72 h of treatment with PrP90–231 (1 μM) induced the shrinkage of CGC neuronal bodies and a complete disruption of the neurite net (Fig. 2b, right panels). Noteworthy, the severity of the neuronal damage was significantly less pronounced in pure CGCs, showing the presence of neurons with spared morphology (arrows in Fig. 2b) and a still appreciable neurite net. Moreover, phase contrast images evidence that CGCs comprise most of dead cells, while glial cells did not show appreciable signs of toxicity.

To confirm this observation and discriminate CGCs from astrocyte and microglia growing underneath the neurite network, we analyzed by immunocytofluorescence the neuronal population contained in the glia-enriched CGC cultures in basal and PrP90–231-treated (72 h) conditions, using the neuron-specific anti- β III-tubulin monoclonal antibody (Banelli et al. 2015). Cultures were counterstained with the nuclear dye DAPI to evidence nuclear condensation or fragmentation and identify astrocytes (larger nuclei of β III-tubulin⁻ cells) (Fig. 3). Untreated cells showed the presence of a dense neuritic network that connects CGCs, whose bodies appears ovoid and without signs of nuclear condensation or

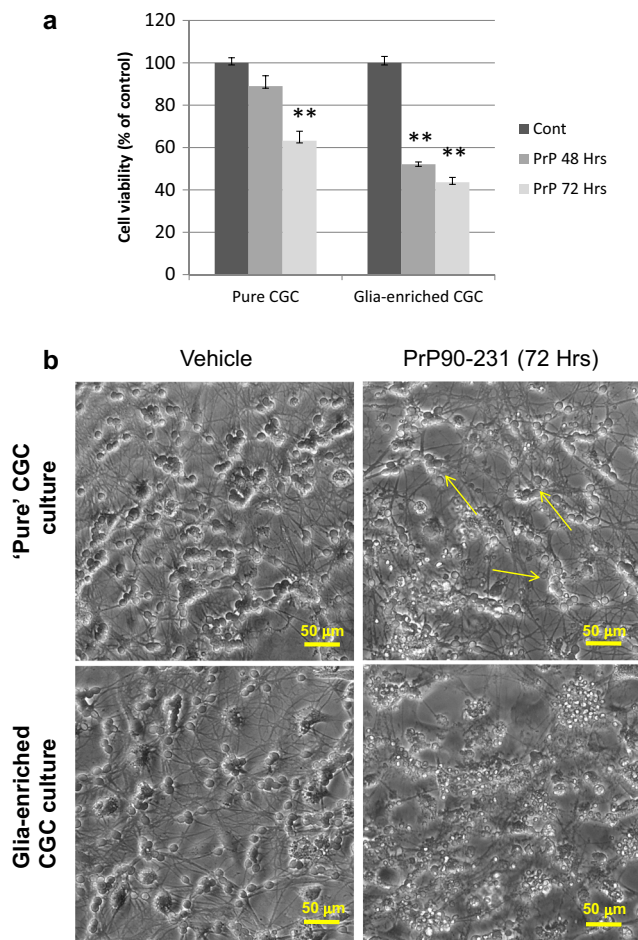


Fig. 2 PrP90–231 toxicity in “pure” and glia-enriched CGCs. **a** Pure and glia-enriched CGCs were treated with vehicle (control) or with PrP90–231 1 μ M for 48 and 72 h. Cell viability was measured by MTT reduction test and expressed as loss of viability in comparison with vehicle-treated controls. Glia-enriched CGCs are significantly more sensitive to PrP90–231 than pure CGCs. Values have been obtained from at least three experiments in quadruplicate. $**p < 0.01$ vs. respective control. **b** Pure and glia-enriched CGCs were treated with PBS (vehicle) and PrP90–231 1 μ M; after 72 h, cultures were photographed by phase-contrast microscopy (objective lens: C PLAN 10 \times 18; scale bar = 50 μ m). The treatment with PrP90–231 caused neuronal condensation shrinkage that, although already evident in pure CGCs (arrows indicate viable neurons), was significantly stronger in glia-enriched CGCs

fragmentation (Fig. 3, upper panels). Treatment with PrP90–231 produced dramatic disruption of neurites in β III-tubulin⁺ cells that also showed condensed apoptotic nuclei, indicating that CGCs are strongly and selectively damaged by PrP90–231 (Fig. 3, lower panels). In contrast, larger nuclei belonging to glial cells, which do not express β III-tubulin, are not condensed or fragmented by PrP90–231 treatment. Altogether, these data indicate that per se the presence of glial cells is not detrimental for CGC viability in vitro and that the exposure of glia-enriched CGC cultures to PrP90–231 induced a specific toxicity on the neuronal component that is significantly higher than what exerted on pure CGC cultures.

PrP90–231 Elicits Fast, Transient $[Ca^{++}]_i$ Peak, Followed by Prolonged Increase of $[Ca^{++}]_i$ in Glia-Enriched CGCs

Sustained increase of cytosolic $[Ca^{++}]_i$, through the activation of NMDA/AMPA glutamatergic receptor, triggers PrP90–231-dependent toxicity in pure CGC cultures, although, under these culturing setting, no rapid transient increase of $[Ca^{++}]_i$ was significantly appreciable (Thellung et al. 2013). Here, we verified whether the presence of glia within CGC cultures may potentiate the alterations of $[Ca^{++}]_i$ homeostasis induced by PrP90–231. To this aim, we measured $[Ca^{++}]_i$ by live cell fluorimetry using the Ca^{++} -sensitive probe Oregon Green (OG), seeking either for fast responses or for more sustained and long-lasting increase of $[Ca^{++}]_i$ after treatment with PrP90–231. Recordings were performed in individual cerebellar granules or type I astrocytes identified according their size and shape; in particular, we recorded fluorescence variations during the first 2 min (Fig. 4) or after 5 (Fig. 5) and 24 h (not shown) of treatment with PrP90–231 (1 μ M). We report $[Ca^{++}]_i$ increase as median difference in cell fluorescence after treatment and as percentage of cells showing fluorescence increase (Table 1). Differently from what observed in neurons from pure CGC cultures that did not show short term changes in OG fluorescence, granule cells from glia-enriched CGC cultures showed a rapid and transient increase of $[Ca^{++}]_i$ that was followed by a return to basal level (within 1–2 min) (Fig. 4a). On the other hand, in astrocytes, PrP90–231 induced a fast and transient $[Ca^{++}]_i$ increase that was detectable in both culture conditions. In detail, in glia-enriched CGC cultures, PrP90–231 induced a transient $[Ca^{++}]_i$ increase in 20% of neurons and 70% of astrocytes that was estimated about 80 and 70% over basal, respectively (Fig. 4b).

Noteworthy, different cellular mechanisms led to the fast $[Ca^{++}]_i$ increase in granule neurons and astrocytes. The incubation of glia-enriched CGC cultures in Ca^{++} -free medium fully abolished the ability of PrP90–231 to generate fast $[Ca^{++}]_i$ increase in neurons and strongly reduced the response in astrocytes, but the treatment with Cd^{++} , a non-selective blocker of voltage-sensitive calcium channels prevented $[Ca^{++}]_i$ in neurons only (Table 1). Altogether, these data indicate that PrP90–231 stimulates a rapid and transient Ca^{++} influx from the extracellular compartment in granule neurons and astrocytes, but only in CGCs it was mediated by the opening of voltage-gated calcium channels (Table 1). To better understand whether high glia content in CGC cultures interfere with PrP90–231-dependent sustained increase of $[Ca^{++}]_i$ in neurons, we measured, by live cell fluorimetry, OG fluorescence in pure and glia-enriched CGCs after 5 h of exposure to PrP90–231 (Fig. 5). The treatment with PrP90–231 produced a net increase $[Ca^{++}]_i$ in cerebellar neurons significantly higher in glia-enriched cultures (+100% of control cells) than in pure CGCs (+25%). These data indicate that the presence of

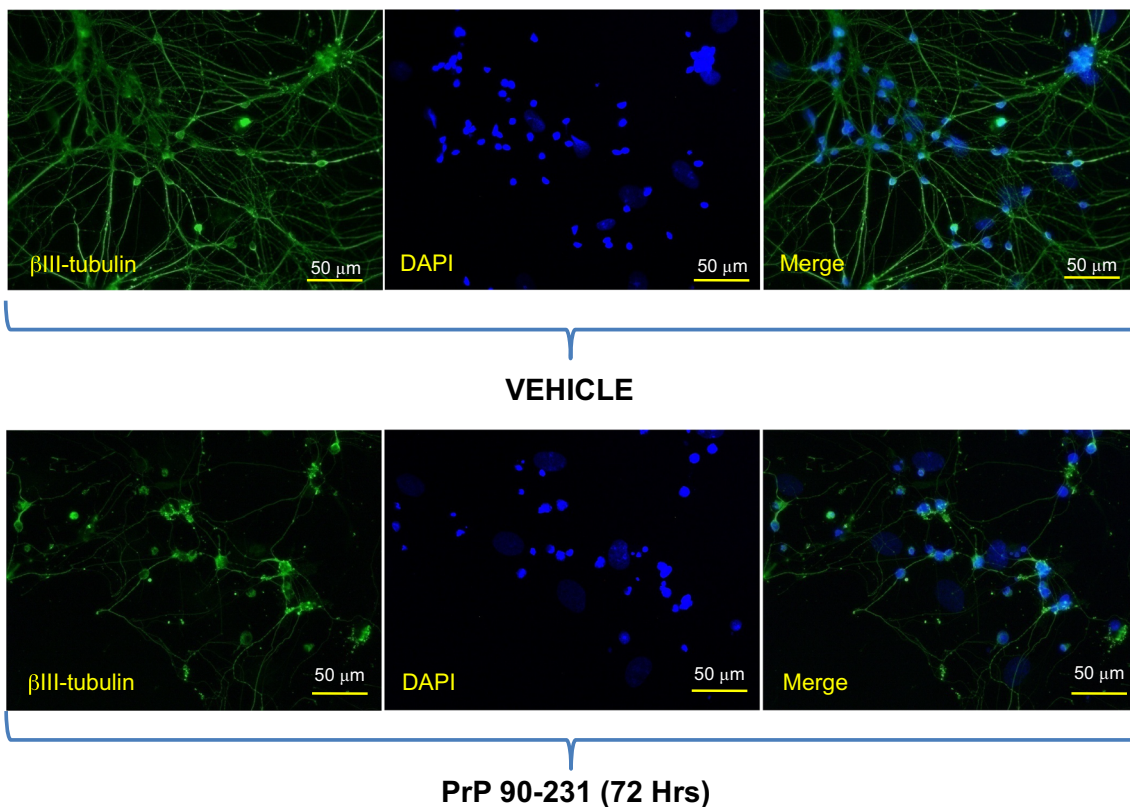


Fig. 3 Evaluation by immunostaining of PrP90–231 neurotoxicity. Immunostaining of glia-enriched CGCs for β III-tubulin after 72 h of treatment with PrP90–231 1 μ M (lower panels) or vehicle (upper panels) was performed to show the integrity of CGC neurite net. DAPI nuclear staining was used to evidence shape and condensation of nuclei (objective lens: HC PL Fluotar 20X/0.50; scale bar = 50 μ m). Upper panels show

that in control CGCs, β III-tubulin stains a well-distributed net without evidencing significant condensed or disaggregating areas. Cultures that have been treated for 3 days with PrP90–231 (lower panels) evidenced appreciable hallmarks of neurite β III-tubulin clustering in cell bodies and neuritis, disaggregation of the net, and appearance of condensed nuclei

high amount of glial cells increases cerebellar granules sensitivity to cytosolic Ca^{++} homeostasis alterations induced by PrP90–231, that represent a molecular basis for the striking higher neurotoxicity observed in glia-enriched CGC cultures. $[Ca^{++}]_i$ measurement was performed also after 24 h of PrP90–231 treatment in glia-enriched CGCs, but in these conditions, neuronal viability was deeply affected hampering the loading with OG and preventing the measurements (data not shown).

PrP90–231 Stimulates NO Production Through iNOS Expression and Upregulates PHOX Expression in Glia-Enriched CGC Cultures

The production of oxygen and nitrogen radical species from activated glial cells contributes to neuronal death induced by PrP^{Sc} and prion-derived amyloidogenic peptides (Brown et al. 1998; Garcao et al. 2006; Villa et al. 2016b). We previously reported that PrP90–231 stimulates the production of NO, PGE₂, CCL5, and monocyte stimulating factors from both astrocytes and microglia (Thellung et al. 2007a; Thellung et al. 2007b; Villa et al. 2016b). Thus, in light of the increased

neurotoxic activity of PrP90–231 observed in the presence of glia, we tested whether a sustained inflammatory response involving the production of oxygen/nitrogen reactive species could represent a molecular correlate of the neurotoxic activity exerted by glial cells on CGCs in response to PrP90–231. First, we evaluated the production of NO in pure and glia-enriched CGC cultures in basal conditions and after exposure to PrP90–231. To this purpose, Griess assay was used to calculate the amount of NO released by the different cell cultures, after 24, 48, and 72 h of treatment with PrP90–231 (1 μ M) (Fig. 6a). Although PrP90–231 increased NO release in both culture conditions, in pure CGCs 3 days of treatment with PrP90–231 were required to observe a statistically significant increase of NO release (Fig. 6a); conversely, glia-enriched CGCs showed a significant increase in release of NO already after 24 h, and exceeded of more than threefold NO released from PrP90–231-treated pure CGC cultures at any tested times. Remarkably, NO production from glia-enriched cultures was steadily sustained by prolonging the treatment time, overcoming, after 3 days of exposure to the peptide, of almost sevenfold NO release in the absence of treatment. To further evidence the production of radical species induced by glial

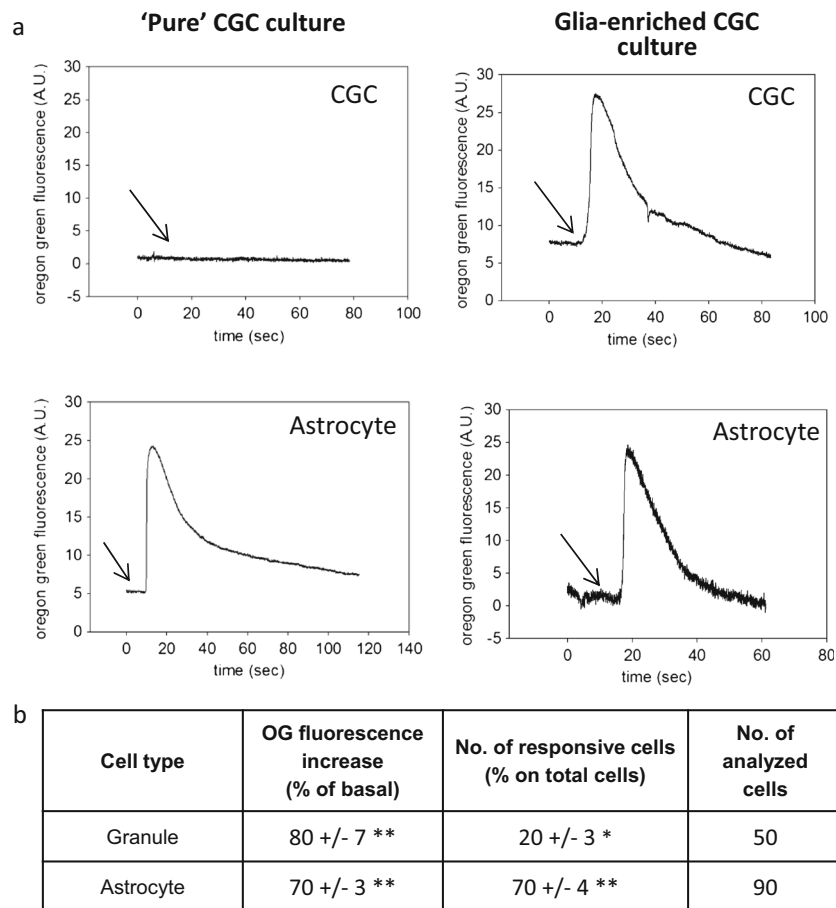


Fig. 4 Measurement of rapid $[Ca^{++}]_i$ increase in CGCs exposed to 90–231. **a** “Pure” and glia-enriched CGCs, seeded on glass coverslips, were loaded with calcium-sensitive fluorescent probe Oregon green (OG) for 15 min. Cells were treated with PBS (basal, not shown) or PrP90–231 (1 μ M) (see *arrows*) and OG fluorescence monitored under single cell fluorimeter. Before the addition of PBS or the peptide, cellular OG fluorescence was measured to determine the baseline in resting conditions. Fluorimetric analysis was carried on granule cells and in glial cells that, basing their large area and being microglial cells relatively less represented, were assumed as type I astrocytes.

Fluorescence analysis reports that 1–2 min of treatment with PrP90–231 1 μ M evoked a rapid increase, followed by a rapid return to baseline, without evidencing plateau phases. $[Ca^{++}]_i$ shift was observed in granule and glial cells without evidencing significant differences in pattern. **b** The table reports a quantification of $[Ca^{++}]_i$ increase (calculated at the peak) and the percent of cells that showed it. Values of $[Ca^{++}]_i$ increase have been calculated as OG fluorescence (in arbitrary units) and expressed as percent of OG fluorescence increase with respect of PBS-treated cells. ** $p < 0.01$ vs. untreated cells

cells, we measured by immunoblotting the expression of iNOS and the phagocytic NADPH oxidase (PHOX) in both pure and glia-enriched CGC cultures and the modulatory effects of PrP90–231. Control and PrP90–231-treated (1 μ M, for 24 h) cultures were analyzed for the expression of iNOS and PHOX catalytic subunit gp91^{phox} (NOX2) (Fig. 6b) and the results from three independent experiments quantified by densitometry (Fig. 6c, d). In basal conditions, both purified and glia-enriched CGC cultures did not express iNOS (Fig. 6b, c), indicating that basal level of NO is not dependent on the activity of iNOS. Conversely, untreated cells express PHOX in both pure and glia-enriched CGC cultures, although in the latter condition, the enzyme was significantly upregulated. PrP90–231 strongly induced iNOS expression in glia-enriched CGC culture only, while it produced a significant increase of PHOX expression in both pure and glia-enriched

CGC cultures (Fig. 6b, d). Moreover, in glia-enriched cultures, iNOS expression induced by PrP90–231 treatment occurred mainly in microglia rather than in astrocytes, as shown by double immunocytofluorescence experiments (Fig. 7a, b). Hence, we explored the possibility to quantify the extent of damage that the reactive species produced by activated microglia in cerebellar cultures could induce on neuronal structures. Among the hallmarks of oxidative stress linked with progression of neurodegenerative conditions, the aldehyde 4-dihydroxynonenal (HNE) produced by membrane lipid peroxidation (Castellani et al. 2002; Zarkovic 2003) is able to form adducts with cellular proteins (Zhang et al. 2017). Both pure and glia-enriched cerebellar granule cultures were treated for 24 h with PrP90–231 (1 μ M) and analyzed by Western blot and immunocytofluorescence for the formation of protein adducts with the aldehyde (Perluigi et al. 2005),

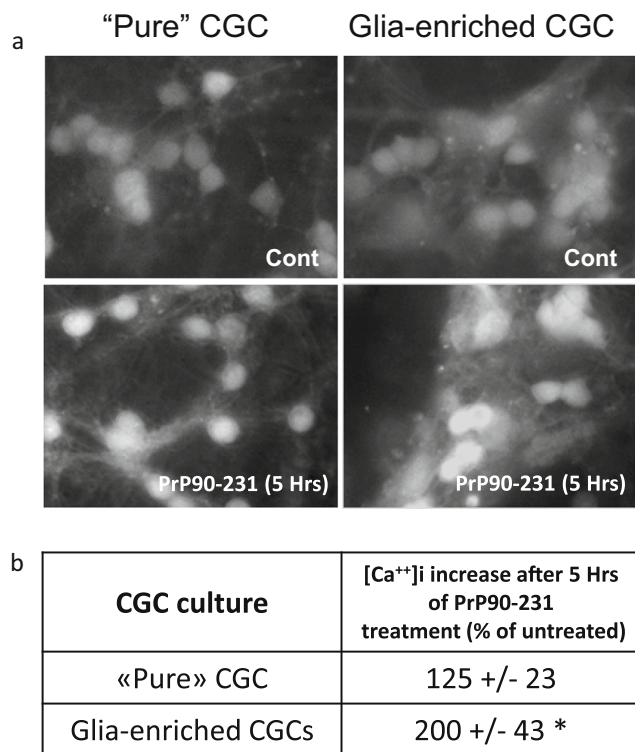


Fig. 5 Measurement of [Ca⁺⁺]_i in CGCs after prolonged treatment with PrP90–231. **(a)** [Ca⁺⁺]_i was measured by OG fluorescence in “pure” and “glia-enriched” CGC cultures after 5 h of treatment with PBS (control) or PrP90–231 (1 μM). Live cell images were acquired from at least 40 granule neurons from each treatment, and the intensity of OG fluorescence was calculated as pixel intensity; values were expressed as % of increase in comparison with untreated samples. The treatment with PrP90–231 induces [Ca⁺⁺]_i increase that was significantly higher in glia-enriched than what observed in pure CGCs. **(b)** Quantification of [Ca⁺⁺]_i increase reported as percent of control cell level. **p* < 0.05 vs. untreated cells

using an anti-HNE antibody (Fig. 8). To better evidence which cell subpopulation primary is mainly affected by HNE production, we counterstained the cultures with monoclonal antibody against βIII-tubulin, expressed in neuronal cytoskeleton. In pure CGC cultures (Fig. 8a, upper panels) a net difference in HNE adducts was observed in control vs. PrP90–231-treated cultures; glial-enriched GCG (Fig. 8a, lower panels) evidenced a higher amount of HNE labeling already detectable in untreated conditions and further increased by exposure to PrP90–231. Noteworthy, HNE distribution, and thus membrane lipid peroxidation, was mostly detectable in neurons as shown by the co-expression of βIII-tubulin. To better quantify the extent of lipid peroxidation induced by PrP90–231, we measured, by Western blot, the expression of HNE-protein adducts in pure or glial-enriched cerebellar granule cells, before and after 24 h of PrP90–231 treatment (Fig. 8b, c). Immunoblotting results are in accordance with immunofluorescence experiments, showing that glial enrichment of CGC cultures, per se, produced an increase of HNE-bound proteins, which was further significantly stimulated by PrP90–231.

Taken together, these data indicate that the glial component (and in particular microglia) within CGC cultures is highly reactive to PrP90–231 in terms of increase NO and ROS release through the over-expression of iNOS and PHOX; the augmented oxidative damage on neuronal structures might be, at least in part, responsible for the higher toxicity of PrP90–231 in glia-enriched cerebellar granule cultures.

Pharmacological Modulation of PrP90–231-Induced Ca⁺⁺ Signaling and Neurotoxicity

Treatment of glia-enriched CGC cultures with PrP90–231 causes a rapid increase of [Ca⁺⁺]_i in non-neuronal cells and, in lower percentage, in granules (Table 1). We previously observed that neurons from pure CGCs did not show fast response to PrP90–231 as far as [Ca⁺⁺]_i increase that occurred only after prolonged treatment, via NMDA-dependent mechanism (Thellung et al. 2013). These differences suggest that the contemporary presence of granule neurons, astrocytes, and microglial cells increases calcium-mediated signals by PrP90–231, although it is undetermined if the transient increase in [Ca⁺⁺]_i is derived from PrP90–231 binding or from some still undetermined soluble molecules released from glial cells. To address this issue, we tested whether the pharmacological blockade of NMDA receptor, or the inhibition of NO or prostaglandins release, might affect [Ca⁺⁺]_i peak in neurons or in astrocytes after treatment with PrP90–231 (Table 1). Glia-enriched CGC cultures were incubated with the competitive NMDA receptor antagonist AP-V (100 μM), iNOS inhibitor *N*-ω-nitro-L-arginine (L-NNA) (500 μM), and COX2 inhibitor celecoxib (10 μM), before being exposed to PrP90–231 (1 μM). As shown in Table 1, AP-V, NNA, and celecoxib prevented [Ca⁺⁺]_i rapid increase in granule cells, determining a complete inhibition of Ca⁺⁺ signaling. Conversely, in astrocytes while AP-V was almost completely ineffective, NNA and celecoxib caused a partial, although statistically significant, reduction of [Ca⁺⁺]_i peak, as far as both number of reactive cells and mean fluorescence (Table 1).

A similar live cell imaging technique was employed to estimate the involvement of NMDA activation and free radical release in modulating the steady [Ca⁺⁺]_i increase we observed after prolonged treatment of glial-enriched CGC cultures. To this purpose, glia-enriched CGC cultures were treated with PBS (controls), AP-V (100 μM), and NNA (500 μM) before the addition of PrP90–231 (1 μM for 5 h). [Ca⁺⁺]_i was measured as OG fluorescence and expressed as percentages of untreated granule cells. The results showed that, while in the presence of NNA, PrP90–231 did not elicit increase of [Ca⁺⁺]_i, the treatment with AP-V reduced the stimulatory effect of PrP90–231 of about 60% (data not shown). This suggests that glial cells growing with neurons significantly reduce the direct contribution of NMDA activity in PrP90–231-dependent Ca⁺⁺ signaling and that glial release of NO may hold

Table 1 Pharmacological characterization of $[Ca^{++}]_i$ increase in glia-enriched CGC cultures

Cell types	OG fluorescence increase (% of basal)	Responsive cells (% on total cells)	No. of evaluated cells
Granule cells			
PrP90–231 (1 μ M)	80 \pm 7**	20 \pm 3*	50
PrP90–231 in Ca^{++} -free medium	0 ^{##}	0 ^{##}	30
PrP90–231 + Cd^{++} (50 μ M)	0 ^{##}	0 ^{##}	21
PrP90–231 + AP-V 100 μ M	0 ^{##}	0 ^{##}	14
PrP90–231 + NNA 500 μ M	0 ^{##}	0 ^{##}	42
PrP90–231 + celecoxib 10 μ M	0 ^{##}	0 ^{##}	37
Glial cells			
PrP90–231 (1 μ M)	70 \pm 3**	70 \pm 4**	90
PrP90–231 in Ca^{++} -free medium	28 \pm 6 [#]	14 \pm 2.5 [#]	50
PrP90–231 + Cd^{++} (50 μ M)	43 \pm 6	50 \pm 3	26
PrP90–231 + AP-V 100 μ M	45 \pm 5	75 \pm 6	24
PrP90–231 + NNA 500 μ M	31 \pm 7 [#]	40 \pm 3.5 [#]	50
PrP90–231 + celecoxib 10 μ M	28 \pm 5 [#]	53 \pm 4 [#]	40

Cells were loaded with Oregon green (OG, 6 μ M) and incubated with external solution with or without Ca^{++} , or in the presence of Cd^{++} 50 μ M, L-NNA 500 μ M, AP-V 100 μ M, and celecoxib 10 μ M for 15 min. OG fluorescence was recorded in single live cell (detecting CGCs from astrocytes on the basis of shape and dimension) to set fluorescence baseline. Afterward, cells were treated with PrP90–231 (1 μ M) and OG fluorescence were recorded at $[Ca^{++}]_i$ peak; values are expressed as percent of fluorescence increase compared on baseline and as percent of cells showing calcium response, in comparison with total amount of cells

* $p < 0.05$ and ** $p < 0.01$ vs. control; [#] $p < 0.05$ and ^{##} $p < 0.01$ vs. PrP90–231

the capacity to “switch on” the ability of the peptide to impair intracellular Ca^{++} homeostasis.

To investigate whether $[Ca^{++}]_i$ elevation, induced by PrP90–231 in glia-enriched CGC cultures correlate with the increased toxicity of the peptide, we investigated the relevance of both NMDA receptor activation and the release of free radicals from activated glia to induce CGC degeneration. To this purpose, pure and glia-enriched CGC cultures preincubated with the NMDA receptor antagonist AP-V (100 μ M) or with the iNOS inhibitor L-NNA (500 μ M) were treated with PrP90–231 (1 μ M) and cell viability evaluated after 72 h by MTT assay (Fig. 9a). We show that in pure CGC cultures, AP-V, but not L-NNA, significantly prevented the loss of viability induced by PrP90–231. Conversely, in glia-enriched cultures, the pretreatment with L-NNA strongly prevented the loss of viability induced by PrP90–231, while the treatment with AP-V was almost completely ineffective. It is worth to note that, although the blockade of NMDA receptor in glia-enriched granule neurons inhibits PrP90–231-induced rapid Ca^{++} entry (see Table 1), it did not prevent the toxicity of the peptide. This indicates that in the presence of glial cells releasing high amounts of NO and oxygen radicals, the sensitivity of neurons

to PrP90–231 increases but their fast response in term of $[Ca^{++}]_i$ elevation does not represent the activation of death pathways.

The relevance of the of radical species produced by glial cells in response to PrP90–231 was further confirmed treating glia-enriched CGC cultures with two iNOS inhibitors, L-NNA (500 μ M) and W1400 (5 μ M), the PHOX inhibitor apocynin (100 μ M), or the COX2 inhibitor celecoxib (10 μ M), before the addition of PrP90–231 (1 μ M). Neuronal death was measured using MTT reduction test after 72 h of treatment (Fig. 9b). CGC viability loss induced by PrP90–231 in glia-enriched cultures was counteracted by both the iNOS inhibitors and the PHOX blocker, while celecoxib was ineffective. This suggest that the reduction of the production of NO and superoxide anion O_2^- , effectively lowers neurotoxic effects of PrP90–231 and that glia activation can lead to the formation of a neurotoxic milieu of oxygen and nitrogen reactive species; conversely, COX2-dependent production of prostaglandins seems not essential for the neurotoxicity induced by PrP90–231.

Altogether, these data led us to conceive a *scenario* in which PrP90–231 neurotoxicity comprises (i) a direct

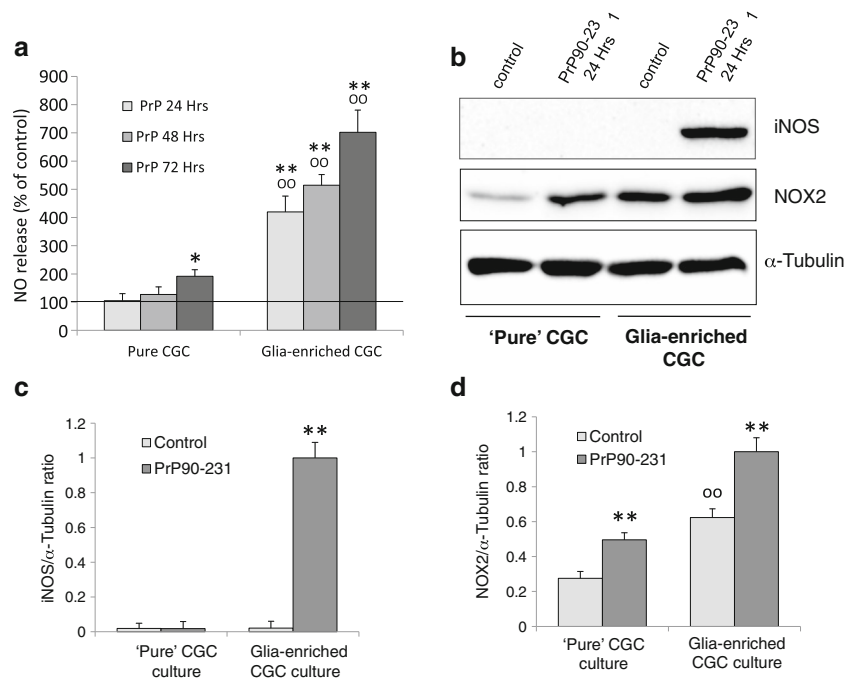


Fig. 6 NO release and PHOX and iNOS expression in “pure” and glia-enriched CGCs induced by PrP90–231. **a** Pure and glia-enriched CGCs were treated with PrP90–231 1 μ M for 24, 48, and 72 h; NO concentration was measured by Griess assay. Values are expressed as percent of NO release on time-matching vehicle-treated cultures (controls, represented in the figure as continue line since it does not change during the experiment), and are derived from the average of three independent experiments performed in quadruplicate. * $p < 0.05$ and ** $p < 0.01$ vs. controls. $^{\circ\circ}p < 0.01$ vs. pure CGC culture. **b** Cells were grown on 60 mm dishes and treated with PBS (control) and PrP90–231 1 μ M for 24 h. Cytoplasmic proteins (50 μ g/lane) were resolved by 10% SDS-PAGE and immunoblotted to detect the expression of iNOS and NOX2 (PHOX catalytic subunit); 10 μ g/lane of each sample was

separately loaded to quantify the expression of α -tubulin. **c** Immunoreactivity for iNOS and **d** NOX2 was quantified by densitometry from three experiments and expressed as iNOS-NOX2/ α -tubulin ratios. In pure CGC, iNOS expression was not detectable in basal conditions and was not appreciably stimulated by the treatment with PrP90–231; conversely, iNOS expression in glia-enriched CGCs, although undetectable in non-stimulated conditions, was significantly induced by the peptide. NOX2 expression, although detectable in pure CGCs, was augmented of onefold in glia-enriched conditions. Moreover, PrP90–231 upregulated NOX2 expression of further 100% in both culturing conditions. ** $p < 0.01$ vs. respective controls; $^{\circ\circ}p < 0.01$ vs. pure CGC culture

excitotoxic activity mediated by NMDA-dependent cytosolic Ca^{++} overloading in neurons and (ii) an indirect toxicity caused by glial activation and the release of free radicals that may produce oxidative stress in neurons or increase neuronal sensitivity to the direct toxicity of peptide.

Discussion

The role of astrocytes and microglia in the pathogenesis of neurodegenerative disorders is an intriguing issue given the structural, nutritional, and defensive roles of these cells. This is particularly true for neurodegenerative amyloidosis in which a spatial and temporal co-localization of amyloid deposits, dying neurons, and recruitment of reactive astrocytes and microglia is reported (Bugiani et al. 2000; Guiroy et al. 1994; Miyazono et al. 1991). Thus, control of glial hyperactivation is nowadays considered a possible valuable common pharmacological strategy to delay the onset or slowdown the progression of central nervous system proteinopathies, including Alzheimer, Parkinson, Huntington, and prion diseases (Eikelenboom et al. 2000; Leszek et al.

2016; McGeer and McGeer 2015). Amyloidogenesis is a process in which the deposition of amyloid fibrils is preceded by the generation of soluble oligomers, insoluble polymers and aggregates, whose relative involvement in neurodegeneration is still not completely defined; rather, intermediate species generated along this process are thought to trigger a chemical cross talk between neurons and glial cells which may ultimately causes neuronal death (Bucciantini et al. 2002; Marella and Chabry 2004). Primary cultures of purified or glia-enriched neurons and, more recently, brain organotypic cultures, are widely used as in vitro models to study the reciprocal influence between neurons and glia in physiological conditions or after the exposition to neurotoxic stimuli, including PrP peptides (Brown 1999; Brown et al. 1998; Falsig et al. 2012). Among non-neuronal cells recruited in response to neurotoxic stimuli, astrocytes and microglia are the most represented within neuronal primary cultures, although they can be kept below 5% in standard culture conditions by the addition of antiproliferative agents. Such restraint is required when research is focused on neurons and the secretive contribution of highly reactive glial cells may hinder a direct neuronal reaction to neurotoxic stimuli. On the other hand,

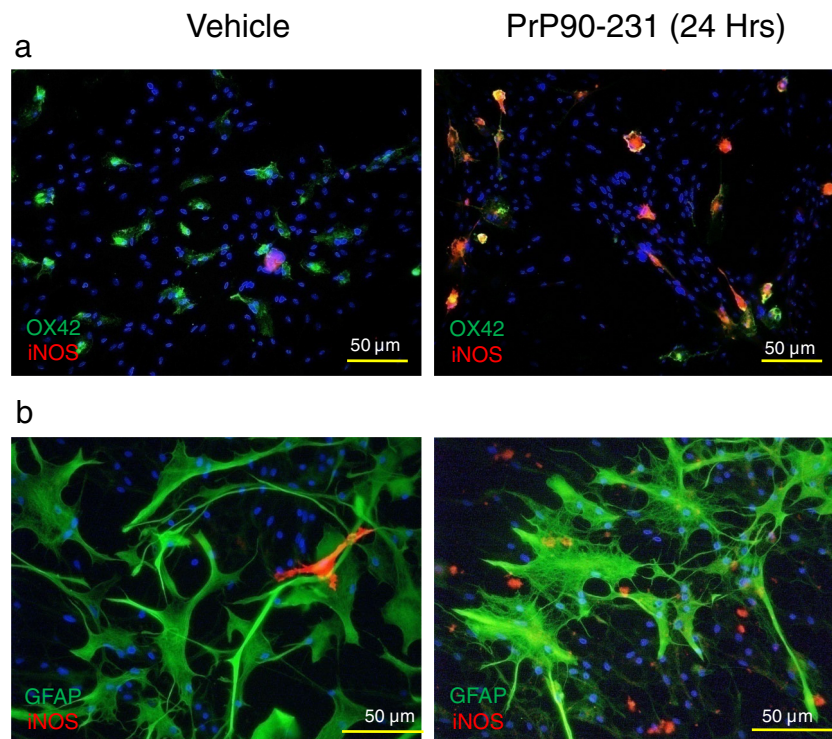


Fig. 7 iNOS expression in astrocytes and microglial cells in glia-enriched CGCs: effect of PrP90–231 treatment. Cultures were treated with PBS (vehicle, left panels) or PrP90–231 (1 µM, right panels) for 24 h before being fixed and subjected to double immunostaining. **a** iNOS/OX42. **b** iNOS/GFAP. AlexaFluor488- and AlexaFluor568-

conjugated antibodies were used to detect immunoreactivity for GFAP/OX42 and for iNOS, respectively. The treatment with PrP90–231 induced a significant expression of iNOS in OX42-positive cells, while no detectable co-localization between iNOS and astrocyte-specific marker GFAP was appreciable (scale bar = 50 µm)

the blockade of glial proliferation in neuronal cultures is a limiting factor when the goal is the characterization of the contribution of non-neuronal cells to the neurotoxic potential of amyloidogenic peptides or drugs (Brown 1999; Dugan et al. 1995; Garcao et al. 2006; Marella and Chabry 2004; Paradisi et al. 2004). In fact, the neurotoxicity of amyloidogenic peptides is likely sustained by a complex proinflammatory cross talk connecting astrocytes/microglia with neurons that cannot be evaluated in neuronal cultures in which glial proliferation is pharmacologically reduced (Marella and Chabry 2004; Marella et al. 2005; Villa et al. 2016a, b). The purpose of the present study was to investigate the differential mechanisms driving the relative contribution of direct and glia-mediated mechanisms of PrP90–231 neurotoxicity, focusing on possible targets for pharmacological therapeutic strategies. We used cerebellar granule cultures in which neuronal-glia interaction is either restrained or enhanced by the control of non-neuronal cell proliferation. We previously demonstrated that PrP90–231 could exert direct neurotoxic effects in pure primary cultures of CGCs through a prolonged activation of NMDA receptors resulting in a sustained elevation of $[Ca^{++}]_i$ (Thellung et al. 2013). Since in these cultures the amount of astrocytes does not exceeded 5% of total cells and microglia is almost

undetectable, NMDA-dependent neurotoxicity of PrP90–231 is likely caused by a direct interaction of the peptide with neurons. Being microglia and astrocytes functionally activated by PrP90–231 to produce proinflammatory and neurotoxic molecules (Thellung et al. 2007b; Villa et al. 2016b), it is reasonable to hypothesize that glial-mediated neurotoxicity of PrP90–231 flanks or possibly overcomes the direct effects of the peptide on neurons. In the present study, we compared the effects of PrP90–231 in pure CGC cultures with cultures in which glial cells were allowed to proliferate for 5 days before adding Ara-C, thus enriching the culture with up 15% of astrocytes and 5% of microglia. This latter model represents a good mean to dissect the heterogeneity of the cellular mechanisms responsible of PrP90–231 neurotoxicity and better mimics the *in vivo scenario* in which the interactions between all these brain cell populations are at the basis of the neurodegenerative processes. We report that PrP90–231 induces cell death in pure CGC cultures, only if the treatment was prolonged for at least 3 days and that it was correlated with a delayed NMDA receptor activation and consequent elevation of $[Ca^{++}]_i$. This observation is in line with reports showing that the neurotoxicity of PrP^{Sc}-related amyloidogenic peptides is dependent on

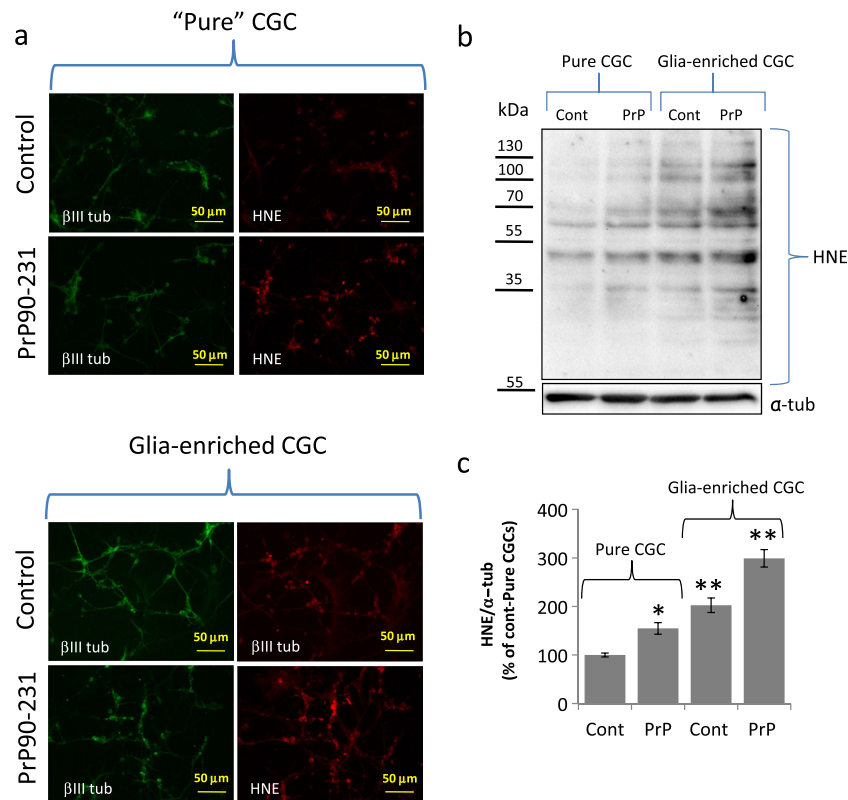


Fig. 8 PrP90–231 induces lipid peroxidation in CGCs. **a** “Pure” (upper panels) and glia-enriched CGCs (lower panels) were plated in 15-mm glass coverslips, and treated with PBS (control) or PrP90–231 1 μ M for 24 h. The expression of neuronal β -III tubulin and lipid peroxidation product 4-hydroxynonenal (HNE) were evaluated by immunofluorescence. Immunoreactivity for β -III tubulin and HNE was evidenced with Alexa Fluor 488- and Alexa Fluor 546- conjugated anti-IgG antibodies, respectively. The amount of HNE was higher in glia-enriched GCG in comparison with pure cultures and was further increased by cell exposure to PrP90–231. (objective lens: HC PL Fluotar 20X/0.50; scale bar = 50 μ m). **b** Pure and glia-enriched CGCs were plated in 60 mm petri dishes and treated with PBS

(control) or PrP90–231 1 μ M for 24 h. Cytoplasmic proteins (50 μ g/lane) were resolved by 10% SDS-PAGE and immunoblotted to detect the amount of HNE adducts to proteins; HNE immunoreactivity was detected throughout the electrophoretic lane. HNE-protein binding was higher in glial-enriched CGCs in comparison to pure CGCs. The treatment with PrP90–231 produced a further increase of HNE adducts in both CGC cultures. To verify equal protein loading, blots were reprobbed with anti- α -tubulin monoclonal antibodies. **c** Immunoreactivity for 4-hydroxynonenal was quantified throughout the lanes by densitometry and expressed as HNE/ α -tubulin ratios and expressed as percent of controls in pure CGCs from three independent experiments. * p < 0.05 and ** p < 0.01 vs. control in pure CGC culture

the direct interaction with neuronal cells that may trigger heterogeneous neurotoxic mechanisms, including alteration of ionic conductance at the plasmamembrane, induction of endoplasmic reticulum stress, or impairment of lysosomal integrity (Ferreiro et al. 2008; Florio et al. 1998; Paulis et al. 2011; Thellung et al. 2011; Thellung et al. 2000b).

However, in cerebellar cultures enriched with high glia content, PrP90–231 exerted a significantly stronger neurotoxic activity. Since cell viability analysis by MTT is based on metabolic measures that evaluate all the cell populations composing the cultures (neurons, astrocytes, microglia), we analyzed cell survival by microscopy visual inspection of cell morphology to discriminate among cell populations. Phase-contrast images of CGCs treated with PrP90–231 showed shrinkage of CGC bodies and the disruption of neurite network, which was more dramatic in glia-enriched CGC cultures. Conversely, no signs of toxicity were observed in glial cells in both culture conditions, confirming that the cytotoxic effects are exerted mainly in

neurons, although significantly enhanced by the presence of glial cells. To investigate the role of glia in mediating PrP90–231 neurotoxicity on CGCs, we evaluated iNOS and PHOX expression in pure and glia-enriched CGCs under basal conditions or after treatment with PrP90–231. Importantly, the expression of iNOS was strongly enhanced after PrP90–231 treatment of mixed neuronal-glial cultures, while it was not induced in pure CGC cultures; such difference of enzymatic expression was confirmed by significant difference in NO release after treatment with PrP90–231. While in pure CGCs, NO release was detectable at low levels only after 3 days of exposure to PrP90–231, unlikely reaching toxic concentrations, it showed a rapid and massive increase in mixed cultures that was highly significant already after 24 h. PHOX expression, although detectable and upregulated by PrP90–231 in both culture conditions, was significantly higher in glia-enriched CGC culture. This suggests that in PrP90–231 treated cultures, the increase of PHOX and iNOS activity causes a higher production of hydroxyl anion O_2^- and

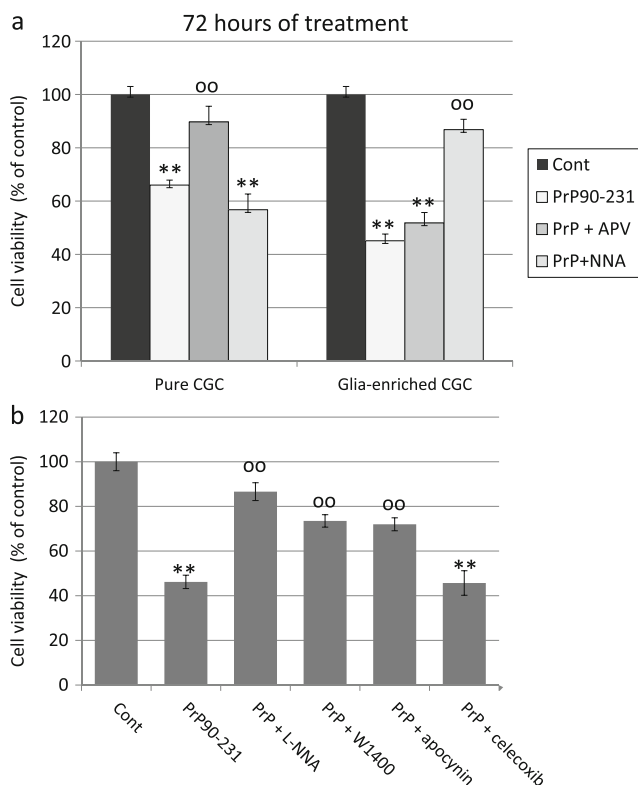


Fig. 9 Pharmacological antagonism of PrP90–231 neurotoxicity in “pure” and glia-enriched CGC cultures. **a** Pure and glia-enriched CGC cultures were incubated with AP-V (100 μ M) and L-NNA (500 μ M) for 30 min before being treated with vehicle (control) or PrP90–231 (1 μ M); cell viability was assessed by MTT assay after 72 h and expressed as loss of viability vs. vehicle-treated controls. PrP90–231 caused a loss of viability of about 35% in pure CGCs, and 55% in glia-enriched CGCs. L-NNA prevented in a highly significant manner glia-enriched CGC loss of viability, but did not protect pure CGCs; oppositely, AP-V antagonized the neurotoxicity of PrP90–231 in pure CGCs only. Values represent the average of three independent experiments in quadruplicate. ** $p < 0.01$ vs. control; ^{oo} $p < 0.01$ vs. PrP90–231. **b** Glia-enriched CGCs were incubated with L-NNA (500 μ M), W1400 (5 μ M), apocynin (100 μ M), and celecoxib (10 μ M), 30 min before cell treatment with vehicle (control) or PrP90–231 (1 μ M); cell viability was measured by MTT assay after 72 h and expressed as loss of viability compared with vehicle-treated controls. PrP90–231 caused a reduction of viability of more than 50% that was significantly inhibited by L-NNA, W1400, and apocynin, while celecoxib was non effective. Values represent the average of three independent experiments performed in quadruplicate

peroxynitrites exposing neurons to highly oxidative *milieu* that is responsible of neuronal death. In particular, the interaction between superoxide anions and NO leads to the formation of neurotoxic peroxynitrite radicals from otherwise harmless NO, enhancing the direct neurotoxicity of amyloid peptides (Mander and Brown 2005). In line with this observation, neuronal oxidative damage, induced by superoxide anions O_2^- and peroxynitrites produced by microglial cells, was previously reported to play a major role in the neurotoxicity during prion diseases (Guentchev et al. 2002; Sorce et al. 2014). The difference in the induction of iNOS and PHOX expression in response

to PrP90–231 between pure and glia-enriched CGC cultures is of particular relevance since highlights different mechanisms on toxicity that are simultaneously activated by PrP90–231. Indeed, we observed that the inhibition of PHOX and/or iNOS activity inhibits PrP90–231 neurotoxicity in glia-enriched CGC culture, but is not effective in pure CGC cultures; on the contrary, NMDA blockade by AP-V exerted neuroprotection in pure CGC cultures, but failed to prevent PrP90–231 neurotoxicity in the presence of glial enrichment. Given that the impairment of intracellular Ca^{++} homeostasis is a major pathway leading to neurodegeneration of CGC cultures (Scorziello et al. 1996, 1997; Thellung et al. 2000b, 2013), we investigated whether glial-dependent increased neurotoxicity of PrP90–231 can produce Ca^{++} homeostasis dysregulation at a higher extent than pure granule cultures. Differently from pure CGC culture in which PrP90–231-induced neuronal death is dependent on a delayed NMDA receptor-dependent increase of $[Ca^{++}]_i$, in the presence of glia, PrP90–231 elicits a rapid increase of $[Ca^{++}]_i$ in both glial and neuronal cells. The kinetics of $[Ca^{++}]_i$ elevation in glia-enriched CGC cultures in response to PrP90–231 is characterized by a rapid recovery to basal $[Ca^{++}]_i$, suggesting that Ca^{++} level alterations are too rapid to induce neurotoxicity. Pharmacological analysis of $[Ca^{++}]_i$ increase showed that Cd^{++} , AP-V and the incubation in Ca^{++} -free medium prevented Ca^{++} increase in all CGCs, indicating that, in the presence of glial cells, the mechanisms controlling Ca^{++} entry from extracellular space, through voltage-gated calcium channels or NMDA receptor activation are readily activated by PrP90–231. It remains to be determined whether the rapid increase of $[Ca^{++}]_i$ in neurons is elicited by direct PrP90–231 binding to glutamatergic receptors, or is induced by some soluble molecules released by glial cells. The latter hypothesis is supported by the observation that $[Ca^{++}]_i$ increase is fully prevented in CGCs, and partly in astrocytes, by the inhibition of iNOS and COX2. In addition to a rapid Ca^{++} movements in a subset of granules, we observed a significant difference in the concentration of $[Ca^{++}]_i$ in CGCs from glia-enriched cultures, after prolonged exposure to PrP90–231. Indeed, after 5 h of treatment with PrP90–231, such increase was detectable also in pure CGCs, but was almost doubled if the treatment was performed in glia-enriched cultures. Since neuroprotection exerted by AP-V was limited to pure CGC cultures, it is likely that glia activation may sustain elevation of $[Ca^{++}]_i$ in neurons in a NMDA receptor-independent manner. Indeed, in the presence of glia, PrP90–231 toxicity is dependent on the overexpression and activation of PHOX and iNOS, resulting in high prooxidative stress as evidenced by HNE protein adducts staining. Importantly, when the neuroinflammatory pathways are activated, glia-dependent neurotoxicity predominates over the direct effects. Thus, the neurotoxic signals activated by PrP90–231 involve multiple pathways acting either directly on neuronal structures or dependent on the activation of glial cells. We propose that in vivo both mechanisms may participate in amyloid peptides induced toxicity and the prevalence of NMDA-

mediated excitotoxicity or glia-mediated oxidative stress is related to the entity of neuroinflammation present. Furthermore, we demonstrate that the pharmacological inhibition of these pathways can prevent neuronal death, supporting that the definition of the mechanisms responsible for the multifactorial neurotoxicity of PrP^{90–231} or other amyloidogenic proteins may provide the basis to develop innovative therapies against CNS proteinopathies.

Moreover, the establishment of culturing approaches allowing the reciprocal modulation among glial cells and neurons allows the identification of relevant intracellular pathways of toxicity induced by amyloid peptides as possible pharmacological targets. Importantly, these pathways may be non-detectable in pure neuronal cultures but become extremely significant *in vivo* where the interactions among neurons and glia are at the basis not only of the physiological functioning but also of the neurodegenerative processes of the brain. Defining the cellular details of this multifactorial neurotoxicity of amyloidogenic peptides might highlight relevant targets to develop novel neuroprotective approaches for CNS proteinopathies.

Acknowledgements The study was supported by grants from the Italian Ministry of University and Research (Accordi di Programma FIRB 2011, project num. RBAP11HSZS) and Compagnia di San Paolo (2013) to TF and Fondo Ricerca Ateneo (FRA, University of Genova) to ST.

Compliance with Ethical Standards Experimental procedures and animal care complied with the EU Parliament and Council Directive of 22 September 2010 (2010/63/EU) and were approved by the Italian Ministry of Health (protocol number 2207-1) in accordance with D.M. 116/1992. All efforts were made to minimize animal suffering and to reduce the number of animal used.

References

- Aguzzi A, O' Connor T (2010) Protein aggregation diseases: pathogenicity and therapeutic perspectives. *Nat Rev Drug Discov* 9:237–248
- Aguzzi A, Barres BA, Bennett ML (2013) Microglia: scapegoat, saboteur, or something else? *Science* 339:156–161
- Arena S, Pattarozzi A, Corsaro A, Schettini G, Florio T (2005) Somatostatin receptor subtype-dependent regulation of nitric oxide release: involvement of different intracellular pathways. *Mol Endocrinol Baltimore, Md* 19:255–267
- Banelli B, Carra E, Barbieri F, Wurth R, Parodi F, Pattarozzi A, Carosio R, Forlani A, Allemanni G, Marubbi D, Florio T, Daga A, Romani M (2015) The histone demethylase KDM5A is a key factor for the resistance to temozolomide in glioblastoma. *Cell Cycle* 14:3418–3429
- Bedard K, Krause KH (2007) The NOX family of ROS-generating NADPH oxidases: physiology and pathophysiology. *Physiol Rev* 87:245–313
- Betmouni S, Perry VH, Gordon JL (1996) Evidence for an early inflammatory response in the central nervous system of mice with scrapie. *Neuroscience* 74:1–5
- Brown DR (1999) Prion protein peptide neurotoxicity can be mediated by astrocytes. *J Neurochem* 73:1105–1113
- Brown DR, Schmidt B, Kretschmar HA (1998) A prion protein fragment primes type 1 astrocytes to proliferation signals from microglia. *Neurobiol Dis* 4:410–422
- Bruce ME, McBride PA, Farquhar CF (1989) Precise targeting of the pathology of the sialoglycoprotein, PrP, and vacuolar degeneration in mouse scrapie. *Neurosci Lett* 102:1–6
- Bucciantini M, Giannoni E, Chiti F, Baroni F, Formigli L, Zurdo J, Taddei N, Ramponi G, Dobson CM, Stefani M (2002) Inherent toxicity of aggregates implies a common mechanism for protein misfolding diseases. *Nature* 416:507–511
- Bugiani O, Giaccone G, Piccardo P, Morbin M, Tagliavini F, Ghetti B (2000) Neuropathology of Gerstmann-Strausler-Scheinker disease. *Microsc Res Tech* 50:10–15
- Castellani RJ, Perry G, Siedlak SL, Nunomura A, Shimohama S, Zhang J, Montine T, Sayre LM, Smith MA (2002) Hydroxynonenal adducts indicate a role for lipid peroxidation in neocortical and brainstem Lewy bodies in humans. *Neurosci Lett* 319:25–28
- Caughey B (2003) Prion protein conversions: insight into mechanisms, TSE transmission barriers and strains. *Br Med Bull* 66:109–120
- Chabry J, Ratsimanohatra C, Sponne I, Elena PP, Vincent JP, Pillot T (2003) *In vivo* and *in vitro* neurotoxicity of the human prion protein (PrP) fragment P118-135 independently of PrP expression. *J Neurosci* 23:462–469
- Chiesa R (2015) The elusive role of the prion protein and the mechanism of toxicity in prion disease. *PLoS Pathog* 11:e1004745
- Chiovitti K, Corsaro A, Thellung S, Villa V, Paludi D, D'Arrigo C, Russo C, Perico A, Ianieri A, Di Cola D, Vergara A, Aceto A, Florio T (2007) Intracellular accumulation of a mild-denatured monomer of the human PrP fragment 90-231, as possible mechanism of its neurotoxic effects. *J Neurochem* 103:2597–2609
- Corsaro A, Thellung S, Russo C, Villa V, Arena S, D'Adamo MC, Paludi D, Rossi Principe D, Damonte G, Benatti U, Aceto A, Tagliavini F, Schettini G, Florio T (2002) Expression in *E. coli* and purification of recombinant fragments of wild type and mutant human prion protein. *Neurochem Int* 41:55–63
- Corsaro A, Thellung S, Villa V, Principe DR, Paludi D, Arena S, Millo E, Schettini D, Damonte G, Aceto A, Schettini G, Florio T (2003) Prion protein fragment 106-126 induces a p38 MAP kinase-dependent apoptosis in SH-SY5Y neuroblastoma cells independently from the amyloid fibril formation. *Ann N Y Acad Sci* 1010:610–622
- Corsaro A, Paludi D, Villa V, D'Arrigo C, Chiovitti K, Thellung S, Russo C, Di Cola D, Ballerini P, Patrone E, Schettini G, Aceto A, Florio T (2006) Conformation dependent pro-apoptotic activity of the recombinant human prion protein fragment 90-231. *Int J Immunopathol Pharmacol* 19:339–356
- Corsaro A, Thellung S, Chiovitti K, Villa V, Simi A, Raggi F, Paludi D, Russo C, Aceto A, Florio T (2009) Dual modulation of ERK1/2 and p 38 MAP kinase activities induced by minocycline reverses the neurotoxic effects of the prion protein fragment 90-231. *Neurotox Res* 15:138–154. doi:10.1007/s12640-009-9015-3
- Corsaro A, Thellung S, Bucciarelli T, Scotti L, Chiovitti K, Villa V, D'Arrigo C, Aceto A, Florio T (2011) High hydrophobic amino acid exposure is responsible of the neurotoxic effects induced by E200K or D202N disease-related mutations of the human prion protein. *Int J Biochem Cell Biol* 43:372–382. doi:10.1016/j.biocel.2010.11.007
- Corsaro A, Thellung S, Villa V, Nizzari M, Aceto A, Florio T (2012a) Recombinant human prion protein fragment 90-231, a useful model to study prion neurotoxicity omics. *J Integr Biol* 16:50–59. doi:10.1089/omi.2011.0038
- Corsaro A, Thellung S, Villa V, Nizzari M, Florio T (2012b) Role of prion protein aggregation in neurotoxicity. *Int J Mol Sci* 13:8648–8669. doi:10.3390/ijms13078648
- DeArmond SJ, Mobley WC, DeMott DL, Barry RA, Beckstead JH, Prusiner SB (1987) Changes in the localization of brain prion proteins during scrapie. *Infect Neurol* 37:1271–1280

- Diack AB, Alibhai JD, Barron R, Bradford B, Piccardo P, Manson JC (2016) Insights into mechanisms of chronic neurodegeneration. *Int J Mol Sci* 17
- Dugan LL, Bruno VM, Amagasu SM, Giffard RG (1995) Glia modulate the response of murine cortical neurons to excitotoxicity: glia exacerbate AMPA neurotoxicity. *J Neurosci* 15:4545–4555
- Eikelenboom P, Rozemuller AJ, Hoozemans JJ, Veerhuis R, van Gool WA (2000) Neuroinflammation and Alzheimer disease: clinical and therapeutic implications. *Alzheimer Dis Assoc Disord* 14(Suppl 1): S54–S61
- Falsig J, Sonati T, Herrmann US, Saban D, Li B, Arroyo K, Ballmer B, Liberski PP, Aguzzi A (2012) Prion pathogenesis is faithfully reproduced in cerebellar organotypic slice cultures. *PLoS Pathog* 8:e1002985
- Ferreiro E, Costa R, Marques S, Cardoso SM, Oliveira CR, Pereira CM (2008) Involvement of mitochondria in endoplasmic reticulum stress-induced apoptotic cell death pathway triggered by the prion peptide PrP(106–126). *J Neurochem* 104:766–776
- Fiala M, Cribbs DH, Rosenthal M, Bernard G (2007) Phagocytosis of amyloid-beta and inflammation: two faces of innate immunity in Alzheimer's disease. *J Alzheimers Dis* 11:457–463
- Florio T, Grimaldi M, Scorziello A, Salmona M, Bugiani O, Tagliavini F, Forloni G, Schettini G (1996) Intracellular calcium rise through L-type calcium channels, as molecular mechanism for prion protein fragment 106–126-induced astroglial proliferation. *Biochem Biophys Res Commun* 228:397–405
- Florio T, Thellung S, Amico C, Robello M, Salmona M, Bugiani O, Tagliavini F, Forloni G, Schettini G (1998) Prion protein fragment 106–126 induces apoptotic cell death and impairment of L-type voltage-sensitive calcium channel activity in the GH3 cell line. *J Neurosci Res* 54:341–352. doi:10.1002/(SICI)1097-4547(19981101)54:3<341::AID-JNR5>3.0.CO;2-G
- Fluharty BR, Biasini E, Stravalaci M, Sclip A, Diomede L, Balducci C, La Vitola P, Messa M, Colombo L, Forloni G, Borsello T, Gobbi M, Harris DA (2013) An N-terminal fragment of the prion protein binds to amyloid-beta oligomers and inhibits their neurotoxicity in vivo. *J Biol Chem* 288:7857–7866
- Forloni G (1996) Neurotoxicity of beta-amyloid and prion peptides. *Curr Opin Neurol* 9:492–500
- Forloni G, Artuso V, La Vitola P, Balducci C (2016) Oligomeropathies and pathogenesis of Alzheimer and Parkinson's diseases. *Mov Disord* 31:771–781. doi:10.1002/mds.26624
- Garcao P, Oliveira CR, Agostinho P (2006) Comparative study of microglia activation induced by amyloid-beta and prion peptides: role in neurodegeneration. *J Neurosci Res* 84:182–193
- Gatta E, Cupello A, Di Braccio M, Grossi G, Ferruzzi R, Roma G, Robello M (2010) New 1,5-benzodiazepine compounds: activity at native GABA(A) receptors. *Neuroscience* 166:917–923
- Ghetti B, Dlouhy SR, Giaccone G, Bugiani O, Frangione B, Farlow MR, Tagliavini F (1995) Gerstmann-Straussler-Scheinker disease and the Indiana kindred. *Brain Pathol* 5:61–75
- Guentchev M, Siedlak SL, Jarius C, Tagliavini F, Castellani RJ, Perry G, Smith MA, Budka H (2002) Oxidative damage to nucleic acids in human prion disease. *Neurobiol Dis* 9:275–281
- Guiroy DC, Wakayama I, Liberski PP, Gajdusek DC (1994) Relationship of microglia and scrapie amyloid-immunoreactive plaques in kuru, Creutzfeldt-Jakob disease and Gerstmann-Straussler syndrome. *Acta Neuropathol* 87:526–530
- Haas J, Storch-Hagenlocher B, Biessmann A, Wildemann B (2002) Inducible nitric oxide synthase and argininosuccinate synthetase: co-induction in brain tissue of patients with Alzheimer's dementia and following stimulation with beta-amyloid 1–42 in vitro. *Neurosci Lett* 322:121–125
- Hong S, Beja-Glasser VF, Nfonoyim BM, Frouin A, Li S, Ramakrishnan S, Merry KM, Shi Q, Rosenthal A, Barres BA, Lemere CA, Selkoe DJ, Stevens B (2016) Complement and microglia mediate early synapse loss in Alzheimer mouse models. *Science* 352:712–716
- Jeffrey M, Goodsir CM, Bruce ME, McBride PA, Farquhar C (1994) Morphogenesis of amyloid plaques in 87V murine scrapie. *Neuropathol Appl Neurobiol* 20:535–542
- Jucker M, Walker LC (2013) Self-propagation of pathogenic protein aggregates in neurodegenerative diseases. *Nature* 501:45–51
- Kayed R, Head E, Thompson JL, McIntire TM, Milton SC, Cotman CW, Glabe CG (2003) Common structure of soluble amyloid oligomers implies common mechanism of pathogenesis. *Science* 300:486–489
- Kim HJ, Chae SC, Lee DK, Chromy B, Lee SC, Park YC, Klein WL, Krafft GA, Hong ST (2003) Selective neuronal degeneration induced by soluble oligomeric amyloid beta protein. *FASEB J* 17: 118–120
- Koenigsnecht J, Landreth G (2004) Microglial phagocytosis of fibrillar beta-amyloid through a beta1 integrin-dependent mechanism. *J Neurosci* 24:9838–9846
- Leszek J, Barreto GE, Gasiorowski K, Koutsouraki E, Avila-Rodriguez M, Aliev G (2016) Inflammatory mechanisms and oxidative stress as key factors responsible for progression of neurodegeneration: role of brain innate immune system. *CNS Neurol Disord Drug Targets* 15:329–336
- Liberski PP, Sikorska B, Lindenbaum S, Goldfarb LG, McLean C, Hainfellner JA, Brown P (2012) Kuru: genes, cannibals and neuropathology. *J Neuropathol Exp Neurol* 71:92–103
- Mallucci GR, White MD, Farmer M, Dickinson A, Khatun H, Powell AD, Brandner S, Jefferys JG, Collinge J (2007) Targeting cellular prion protein reverses early cognitive deficits and neurophysiological dysfunction in prion-infected mice. *Neuron* 53:325–335
- Mander P, Brown GC (2005) Activation of microglial NADPH oxidase is synergistic with glial iNOS expression in inducing neuronal death: a dual-key mechanism of inflammatory neurodegeneration. *J Neuroinflammation* 2:20
- Mandrekar S, Jiang Q, Lee CY, Koenigsnecht-Talboo J, Holtzman DM, Landreth GE (2009) Microglia mediate the clearance of soluble Abeta through fluid phase macropinocytosis. *J Neurosci* 29:4252–4262
- Marella M, Chabry J (2004) Neurons and astrocytes respond to prion infection by inducing microglia recruitment. *J Neurosci* 24:620–627
- Marella M, Gaggioli C, Batoz M, Deckert M, Tartare-Deckert S, Chabry J (2005) Pathological prion protein exposure switches on neuronal mitogen-activated protein kinase pathway resulting in microglia recruitment. *J Biol Chem* 280:1529–1534. doi:10.1074/jbc.M410966200
- McGeer PL, McGeer EG (2015) Targeting microglia for the treatment of Alzheimer's disease. *Expert Opin Ther Targets* 19:497–506
- Miyazono M, Iwaki T, Kitamoto T, Kaneko Y, Doh-ura K, Tateishi J (1991) A comparative immunohistochemical study of Kuru and senile plaques with a special reference to glial reactions at various stages of amyloid plaque formation. *Am J Pathol* 139:589–598
- Monaco S, Zanusso G, Mazzucco S, Rizzuto N (2006) Cerebral amyloid-oses: molecular pathways and therapeutic challenges. *Curr Med Chem* 13:1903–1913
- Montagna P, Gambetti P, Cortelli P, Lugaresi E (2003) Familial and sporadic fatal insomnia. *Lancet Neurol* 2:167–176
- Neniskyte U, Neher JJ, Brown GC (2011) Neuronal death induced by nanomolar amyloid beta is mediated by primary phagocytosis of neurons by microglia. *J Biol Chem* 286:39904–39913
- Notari S, Strammiello R, Capellari S, Giese A, Cescatti M, Grassi J, Ghetti B, Langeveld JP, Zou WQ, Gambetti P, Kretschmar HA, Parchi P (2008) Characterization of truncated forms of abnormal prion protein in Creutzfeldt-Jakob disease. *J Biol Chem* 283: 30557–30565

- Novitskaya V, Bocharova OV, Bronstein I, Baskakov IV (2006) Amyloid fibrils of mammalian prion protein are highly toxic to cultured cells and primary neurons. *J Biol Chem* 281:13828–13836
- Paradisi S, Sacchetti B, Balduzzi M, Gaudi S, Malchiodi-Albedi F (2004) Astrocyte modulation of in vitro beta-amyloid neurotoxicity. *Glia* 46:252–260
- Paulis D, Maras B, Schinina ME, di Francesco L, Principe S, Galeno R, Abdel-Haq H, Cardone F, Florio T, Pocchiari M, Mazzanti M (2011) The pathological prion protein forms ionic conductance in lipid bilayer. *Neurochem Int* 59:168–174
- Pellistri F, Bucciantini M, Relini A, Nosi D, Gliozzi A, Robello M, Stefani M (2008) Nonspecific interaction of prefibrillar amyloid aggregates with glutamatergic receptors results in Ca²⁺ increase in primary neuronal cells. *J Biol Chem* 283:29950–29960
- Perluigi M, Fai Poon H, Hensley K, Pierce WM, Klein JB, Calabrese V, De Marco C, Butterfield DA (2005) Proteomic analysis of 4-hydroxy-2-nonenal-modified proteins in G93A-SOD1 transgenic mice—a model of familial amyotrophic lateral sclerosis. *Free Radic Biol Med* 38:960–968. doi:10.1016/j.freeradbiomed.2004.12.021
- Piccioli P, Porcile C, Stanzione S, Bisaglia M, Bajetto A, Bonavia R, Florio T, Schettini G (2001) Inhibition of nuclear factor-kappaB activation induces apoptosis in cerebellar granule cells. *J Neurosci Res* 66:1064–1073. doi:10.1002/jnr.1251
- Post K, Brown DR, Groschup M, Kretschmar HA, Riesner D (2000) Neurotoxicity but not infectivity of prion proteins can be induced reversibly in vitro. *Arch Virol Suppl*:265–273
- Prusiner SB (1998) Prions Proceedings of the National Academy of Sciences of the United States of America 95:13363–13383
- Puoti G, Bizzi A, Forloni G, Safar JG, Tagliavini F, Gambetti P (2012) Sporadic human prion diseases: molecular insights and diagnosis. *Lancet Neurol* 11:618–628
- Scorziello A, Meucci O, Florio T, Fattore M, Forloni G, Salmona M, Schettini G (1996) Beta 25-35 alters calcium homeostasis and induces neurotoxicity in cerebellar granule cells. *J Neurochem* 66:1995–2003
- Scorziello A, Florio T, Bajetto A, Thellung S, Schettini G (1997) TGF-beta1 prevents gp 120-induced impairment of Ca²⁺ homeostasis and rescues cortical neurons from apoptotic death. *J Neurosci Res* 49:600–607. doi:10.1002/(SICI)1097-4547(19970901)49:5<600::AID-JNR10>3.0.CO;2-Z
- Selkoe DJ, Hardy J (2016) The amyloid hypothesis of Alzheimer's disease at 25 years. *EMBO Mol Med* 8:595–608. doi:10.15252/emmm.201606210
- Serrano-Pozo A, Mielke ML, Gomez-Isla T, Betensky RA, Growdon JH, Frosch MP, Hyman BT (2011) Reactive glia not only associates with plaques but also parallels tangles in Alzheimer's disease. *Am J Pathol* 179:1373–1384
- Sorce S, Nuvolone M, Keller A, Falsig J, Varol A, Schwarz P, Bieri M, Budka H, Aguzzi A (2014) The role of the NADPH oxidase NOX2 in prion pathogenesis. *PLoS Pathog* 10:e1004531
- Sorrentino S, Bucciarelli T, Corsaro A, Tosatto A, Thellung S, Villa V, Schinina ME, Maras B, Galeno R, Scotti L, Creati F, Marrone A, Re N, Aceto A, Florio T, Mazzanti M (2012) Calcium binding promotes prion protein fragment 90-231 conformational change toward a membrane destabilizing and cytotoxic structure. *PLoS One* 7:e38314. doi:10.1371/journal.pone.0038314
- Soto C, Estrada L, Castilla J (2006) Amyloids, prions and the inherent infectious nature of misfolded protein aggregates. *Trends Biochem Sci* 31:150–155
- Thellung S, Florio T, Corsaro A, Arena S, Merlino M, Salmona M, Tagliavini F, Bugiani O, Forloni G, Schettini G (2000a) Intracellular mechanisms mediating the neuronal death and astrogliosis induced by the prion protein fragment 106-126. *Int J Dev Neurosci* 18:481–492
- Thellung S, Florio T, Villa V, Corsaro A, Arena S, Amico C, Robello M, Salmona M, Forloni G, Bugiani O, Tagliavini F, Schettini G (2000b) Apoptotic cell death and impairment of L-type voltage-sensitive calcium channel activity in rat cerebellar granule cells treated with the prion protein fragment 106-126. *Neurobiol Dis* 7:299–309
- Thellung S, Corsaro A, Villa V, Venezia V, Nizzari M, Bisaglia M, Russo C, Schettini G, Aceto A, Florio T (2007a) Amino-terminally truncated prion protein PrP90-231 induces microglial activation in vitro. *Ann N Y Acad Sci* 1096:258–270. doi:10.1196/annals.1397.092
- Thellung S, Villa V, Corsaro A, Pellistri F, Venezia V, Russo C, Aceto A, Robello M, Florio T (2007b) ERK1/2 and p38 MAP kinases control prion protein fragment 90-231-induced astrocyte proliferation and microglia activation. *Glia* 55:1469–1485
- Thellung S, Corsaro A, Villa V, Simi A, Vella S, Pagano A, Florio T (2011) Human PrP90-231-induced cell death is associated with intracellular accumulation of insoluble and protease-resistant macroaggregates and lysosomal dysfunction. *Cell Death Dis* 2:e138. doi:10.1038/cddis.2011.21
- Thellung S, Gatta E, Pellistri F, Corsaro A, Villa V, Vassalli M, Robello M, Florio T (2013) Excitotoxicity through NMDA receptors mediates cerebellar granule neuron apoptosis induced by prion protein 90-231 fragment. *Neurotox Res* 23:301–314
- Tousseyn T, Bajsarowicz K, Sanchez H, Gheyara A, Oehler A, Geschwind M, DeArmond B, DeArmond SJ (2015) Prion disease induces Alzheimer disease-like neuropathologic changes. *J Neuropathol Exp Neurol* 74:873–888
- Van Everbroeck B, Dobbeleir I, De Waele M, De Leenheir E, Lubke U, Martin JJ, Cras P (2004) Extracellular protein deposition correlates with glial activation and oxidative stress in Creutzfeldt-Jakob and Alzheimer's disease. *Acta Neuropathol* 108:194–200
- Villa V, Thellung S, Bajetto A, Gatta E, Robello M, Novelli F, Tasso B, Tonelli M, Florio T (2016a) Novel celecoxib analogues inhibit glial production of prostaglandin E2, nitric oxide, and oxygen radicals reverting the neuroinflammatory responses induced by misfolded prion protein fragment 90-231 or lipopolysaccharide. *Pharmacol Res* 113:500–514. doi:10.1016/j.phrs.2016.09.010
- Villa V, Thellung S, Corsaro A, Novelli F, Tasso B, Colucci-D'Amato L, Gatta E, Tonelli M, Florio T (2016b) Celecoxib inhibits prion protein 90-231-mediated pro-inflammatory responses in microglial cells. *Mol Neurobiol* 53:57–72
- Weldon DT, Rogers SD, Ghilardi JR, Finke MP, Cleary JP, O'Hare E, Esler WP, Maggio JE, Mantyh PW (1998) Fibrillar beta-amyloid induces microglial phagocytosis, expression of inducible nitric oxide synthase, and loss of a select population of neurons in the rat CNS in vivo. *J Neurosci* 18:2161–2173
- Williams A, Lucassen PJ, Ritchie D, Bruce M (1997) PrP deposition, microglial activation, and neuronal apoptosis in murine scrapie. *Exp Neurol* 144:433–438
- Xiao X, Yuan J, Qing L, Cali I, Mikol J, Delisle MB, Uro-Coste E, Zeng L, Abouelsaad M, Gazgalis D, Martinez MC, Wang GX, Brown P, Ironside JW, Gambetti P, Kong Q, Zou WQ (2014) Comparative study of prions in iatrogenic and sporadic Creutzfeldt-Jakob disease. *J Clin Cell Immunol* 5:240
- Xie WL, Shi Q, Zhang J, Zhang BY, Gong HS, Guo Y, Wang SB, Xu Y, Wang K, Chen C, Liu Y, Dong XP (2013) Abnormal activation of microglia accompanied with disrupted CX3CR1/CX3CL1 pathway in the brains of the hamsters infected with scrapie agent 263K. *J Mol Neurosci* 51:919–932
- Zarkovic K (2003) 4-hydroxynonenal and neurodegenerative diseases. *Mol Asp Med* 24:293–303
- Zhang S, Eitan E, Mattson MP (2017) Early involvement of lysosome dysfunction in the degeneration of cerebral cortical neurons caused by the lipid peroxidation product 4-hydroxynonenal. *J Neurochem* 140:941–954. doi:10.1111/jnc.13957